

Osseous Anatomy and Microanatomy of the Lunate

2

Chong Jin Yeo, Gregory Ian Bain,
and Egon Perilli

Introduction

The name of the lunate bone derives from the “crescent-shaped” (Latin: *lunatus*), from Latin *luna* (“moon”), from the bone’s resemblance to a crescent moon. The lunate has been described as the keystone of the wrist. It is the “intercalated” segment of the intercalated proximal carpal row.

An understanding of the normal anatomy and variants is of value before delving into the pathological anatomy.

C.J. Yeo, MBChB, MRCS, MMed, FAMS
Hand and Microsurgery Section, Department of
Orthopedic Surgery, Tan Tock Seng Hospital,
11 Jalan Tan Tock Seng, Singapore 308433,
Singapore

G.I. Bain, MBBS, FRACS, FA(Ortho)A, PhD (✉)
Professor, Upper Limb and Research, Department of
Orthopedic Surgery, Flinders University and Flinders
Medical Centre, Bedford Park, Adelaide,
SA, Australia
e-mail: greg@gregbain.com.au

E. Perilli, PhD (Bioeng), MSc (Phys)
Medical Device Research Institute, School of
Computer Science, Engineering and Mathematics,
Flinders University, 1284 South Rd, Clovelly Park,
SA 5082, Australia

Gross Anatomy of the Normal Lunate

Dr. Henry Gray, in 1858, described the lunate in his classic text “Anatomy: Descriptive and Surgical” as follows:

“The *Semi-lunar* bone may be distinguished by its deep concavity and crescentic outline. It is situated in the centre of the upper range of the carpus, between the scaphoid and cuneiform. Its *superior surface*, convex, smooth and quadrilateral in form, articulates with the radius. Its *inferior surface* is deeply concave, and of greater extent from before backwards, than transversely; it articulates with the head of the os magnum, and by a long narrow facet (separated by a ridge from the general surface) with the unciform bone. Its *anterior* or *palmar* and *posterior* or *dorsal surface* are rough, for the attachment of ligaments, the former being broader, and of somewhat rounded form. The *external surface* presents a narrow, flattened, semi-lunar facet, for articulation with the scaphoid. The *internal surface* is marked by a smooth, quadrilateral facet, for articulation with the cuneiform (Fig. 2.1).

To ascertain to which hand this bone belongs, hold it with the dorsal surface upwards, and the convex articular surface backwards; the quadrilateral articular facet will then point to the side to which the bone belongs.

Articulations. With five bones: the radius above, os magnum and unciform below, scaphoid and cuneiform on either side.”

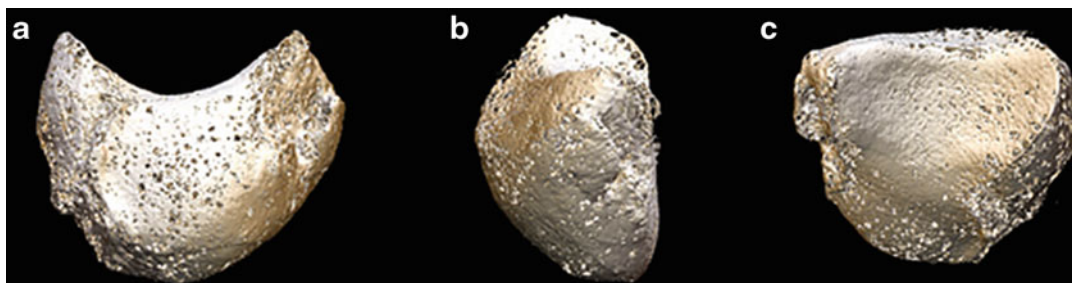


Fig. 2.1 Micro-CT 3D images of the normal lunate from a (a) radial view, (b) volar view, and (c) distal view. Reproduced with permission from Low S, Bain GI, Findlay DM, Eng K, Perilli E, External and internal bone

micro-architecture in normal and Kienböck's lunates: A whole-bone micro-computed tomography study. *J Orthop Res* 2014; 32 (6): 826–833. © 2014 Orthopedic Research Society. Published by Wiley Periodicals, Inc.

In addition to some changes in nomenclature of the bones, this description is still very much applicable today.

The lunate is cartilaginous at birth and usually has one ossification center that begins to ossify during the fourth year [1]. Ossification has been noted to take place from 1.5 to 7 years of age in boys, and between 1 and 6 years of age in girls. There have also been observations of double-ossification centers in the lunate.

Several accessory bones can be associated with the lunate. Accessory bones, if present, usually are the result of a secondary or an additional ossification center that does not fuse with the associated bone. These have been associated with the lunate: the os epilunatum (os centrale II), the os hypolunatum (os centrale III), the os hypotriquetrum, the os epitriquetrum (epipyramis, os centrale IV), and the os triangulare (os intermedium antebrachii, os triquetrum secundarium) [2]. The os epilunatum is located between the lunate, scaphoid, and capitate, along the distal border of the scaphoid and lunate. The os hypolunatum is located between the lunate and the capitate, just ulnar to the site of the os epilunatum. The os hypotriquetrum is located in the vicinity of the lunate, capitate, proximal pole of the hamate, and the triquetrum. The os epitriquetrum is located between the lunate, hamate, and triquetrum, just ulnar to the site of the os hypotriquetrum. The os triangulare is located between the lunate, triquetrum, and the distal ulna [2].

The lunate is crescentic, concave distally, and convex proximally. It consists of internally cancellous bone, surrounded by a cortical shell. The dorsal and palmar surfaces where the carpal ligaments attach to are rough. The palmar surface is roughly triangular and is larger and wider than the dorsal portion. The smooth, convex proximal articular surface articulates with the lunate fossa of the distal radius and with a portion of the triangular fibrocartilage on its proximal ulnar aspect. The lateral surface is crescent shaped, flat, and narrow, with a relatively narrow surface area with which it contacts the scaphoid. The medial surface is square or rectangular, and fairly flat, and articulates with the triquetrum. The distal surface is deeply concave and articulates with the proximal portion of the capitate. There are variations noted for the distal articulations that will be touched upon later in the chapter.

Of note, there are no muscle origins or insertions on the lunate, but has a volar and dorsal capsule, and the scapholunate and lunotriquetral ligaments.

Five bones articulate with the lunate: the radius, scaphoid, capitate, hamate, and triquetrum. The lunate articulates with the radius on its proximal surface where it lies in the lunate fossa of the radius, located on the ulnar aspect of the distal radius. The lunate articulates with the scaphoid along the lunate's radial surface, with a relatively small, crescent-shaped articular surface area. The lunate articulates with the capitate dis-

tally, where the proximal pole of the capitate sits in the distal, crescent-shaped articular surface of the lunate. Between the articular surfaces for the triquetrum and the capitate, there usually is a narrow strip of articular surface for articulation with the proximal portion of the hamate. A curved ridge separates the articular surfaces for the hamate and capitate. Contact with the hamate is maximized with ulnar deviation.

Normal Lunate Morphology

Viegas et al. described two types of lunates based on the existence of a distal medial facet. Type I lunates (35%) had no distal medial facet while type II (65%) lunates had a distal medial facet that articulates with the hamate [3] (Fig. 2.2).

Zapico in 1966 categorized lunate morphology into three types (Fig. 2.3) and also noted a relation-

Fig. 2.2 Lunate morphology as described by Viegas. Type I has an absent medial facet, while type II had a medial facet articulating with the hamate

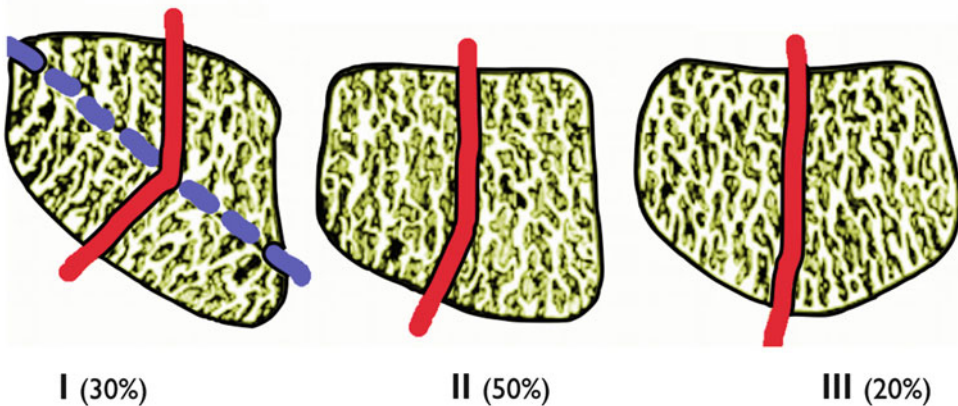
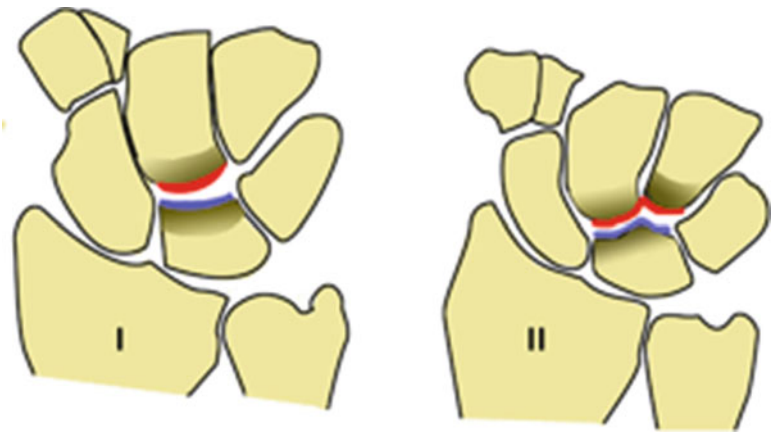


Fig. 2.3 Lunate morphology as described by Zapico. The Zapico type I lunates have a trabecular angulation of greater than 135°, making it less able to tolerate compressive loads and thus at risk for Kienböck's disease. Modified from [4]

ship between the ulnar variance and type of lunate [4, 5]. Type I lunates are trapezoidal in shape and associated with negative ulnar variance. Type II lunates are more rectangular in shape and associated with ulnar neutral wrists. Type III lunates are pentagonal, with two proximal joint surfaces, and found typically with positive ulnar variance.

Wrist Morphology Associated with Kienböck's Disease

There are a number of morphological factors of the lunate, radius, and ulnar that are known to be associated with Kienböck's disease.

Lunate Morphology Associated with Kienböck's Disease

1. There is a higher incidence of Viegas' type I lunates in Kienböck's disease patients as compared to the general population [6–8].
2. Zapico's type I lunate is postulated to be more susceptible to Kienböck's disease due to the potential plane of weakness as the trabecular angulation with greater than 135° is less able to withstand compressive forces [9]. This is based on the studies that trabeculae within the lunate run perpendicular to the proximal and distal articular surfaces [4, 9].

Radius Morphology Associated with Kienböck's Disease

1. Ulnar variance is one of the most commonly cited factors for lunate loading. A short ulna will increase the load on the radial half of the lunate. There are numerous studies to support this mechanism [10–13].
2. A flatter radial inclination with a smaller lunate was noted in patients with Kienböck's disease on their contralateral wrists as compared to the normal population [14].

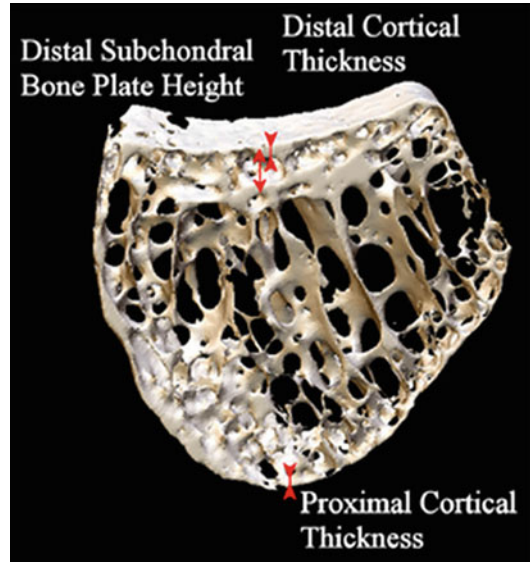


Fig. 2.4 3D micro-CT image demonstrating posterior view of left lunate, with trabeculae spanning from the proximal to the distal subchondral bone plate. Note that the proximal subchondral bone plate is a single layer, which may predispose to a stress fracture of the proximal surface, and it is repeatedly loaded in the same location. Copyright Dr. Gregory Bain

Microstructure of the Normal Lunate

Micro-CT images demonstrate that the lunate has single-layered cortices, except the distal subchondral bone plate that articulates with the capitate [15]. This distal lunate subchondral bone plate was multilayered with each layer separated by short perpendicular bridging trabeculae (Fig. 2.4). We refer to the superficial layer as the primary subchondral bone plate, and then the secondary plate below it [15]. The coronal 3D micro-CT images demonstrated multiple radially arranged trabeculae, spanning from the distally reinforced multilayered subchondral bone plate to the single-layered proximal subchondral bone plate (Fig. 2.5). By spanning from the proximal to the distal subchondral bone plate, they maintain this distance, transmit the load, and maintain the height of the lunate.

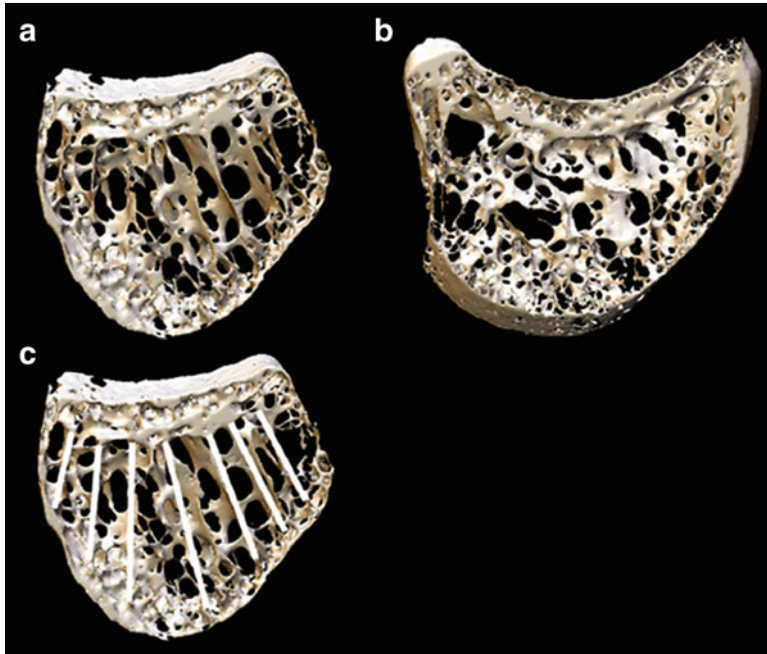


Fig. 2.5 3D micro-CT images, 1 mm thick cross sections of the lunate: (a) coronal section showing radial pattern of the trabeculae, spanning from distal to the proximal subchondral bone plate, (b) sagittal section, and (c) coronal section with radial lines highlighted in *white*, evidencing radial spanning trabeculae. Reproduced with permission

from Low S, Bain GI, Findlay DM, Eng K, Perilli E, External and internal bone micro-architecture in normal and Kienböck's lunates: A whole-bone micro-computed tomography study. *J Orthop Res* 2014; 32 (6): 826–833.© 2014 Orthopedic Research Society. Published by Wiley Periodicals, Inc.

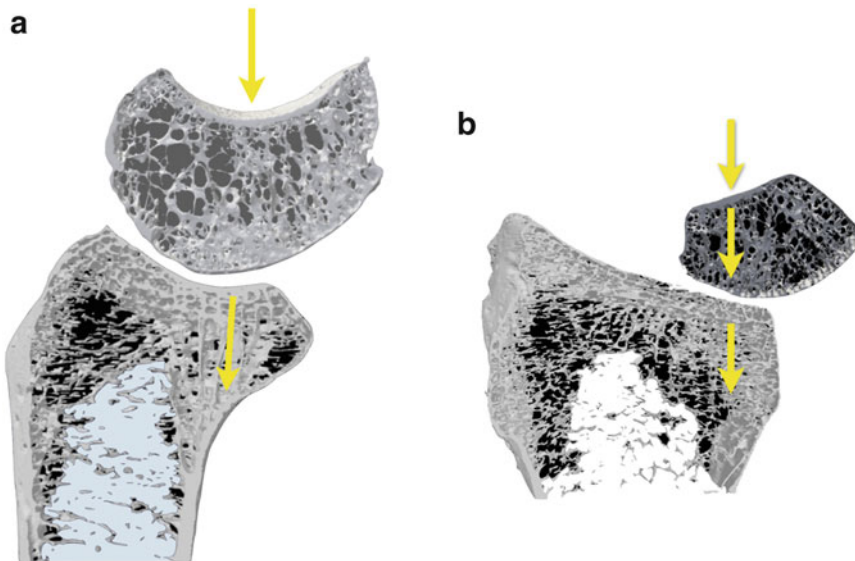


Fig. 2.6 Micro-CT images showing the internal trabeculae and subchondral structures for the lunate and radius. (a) Sagittal view with the *bold arrow* illustrating the loading

force from distal, and the *transparent arrows* showing the thickened trabeculae and subchondral bone. (b) Coronal view. Copyright Dr. Gregory Bain

The subchondral bone is a shock absorber and can be seen morphologically to distribute the joint stresses (Fig. 2.6). Below it, intermediate spanning trabeculae extend from the proximal to the distal articular surfaces and maintain the lunate height. The proximal articular “condyle” is the common site of Kienböck’s disease. It is to be noted that the subchondral bone plate on the convex proximal surface is *only a single layer*, and it is this surface that is prone to the lunate fracture of Kienböck’s disease. The distal multi-layered cortex is self-reinforcing, and typically has a coronal fracture due to the impinging capitate. The main soft-tissue attachments, which include the vascular pedicles, are on the volar and dorsal aspects. Unlike long bones, there is almost no periosteum on the lunate.

Microstructure of the Kienböck’s Lunate

3D micro-CT images reveal that the lunates in Kienböck’s disease had lost the normal crescent shape, and are fractured and fragmented, showing destruction of the bone, with only part of the cortex being present, both proximally and distally. The proximal cortex was more severely fragmented than the distal aspect (Fig. 2.7).

Internal morphology displayed regions of dense trabeculae bone interspersed with regions devoid of bone, with some residual evidence of the distal subchondral bone plate (Fig. 2.8). However, the radially patterned trabeculae that normally span from the distal to the proximal lunate subchondral bone plate were largely absent, due to bone fragmentation and resorption.

The micro-CT demonstrates the sparse pattern of normal lunate, compared to the avascular lunate, in which there are twice as many trabeculae that are thicker ($\times 3$). However, the total bone volume of the lunate is reduced, as a consequence of the bone resorption [4] (Fig. 2.9).

The subchondral bone plate is an important morphological structure that transmits the load, and provides a consistent platform for the articular cartilage. The subchondral bone plate can be compromised by fracture, or it can be eroded such that the articular cartilage has no support (Fig. 2.10).

Histology of the Kienböck’s Lunate

Gross examination demonstrates the ulcerated changes of the articular surface, and the necrotic subchondral bone plate (Fig. 2.11). Histological

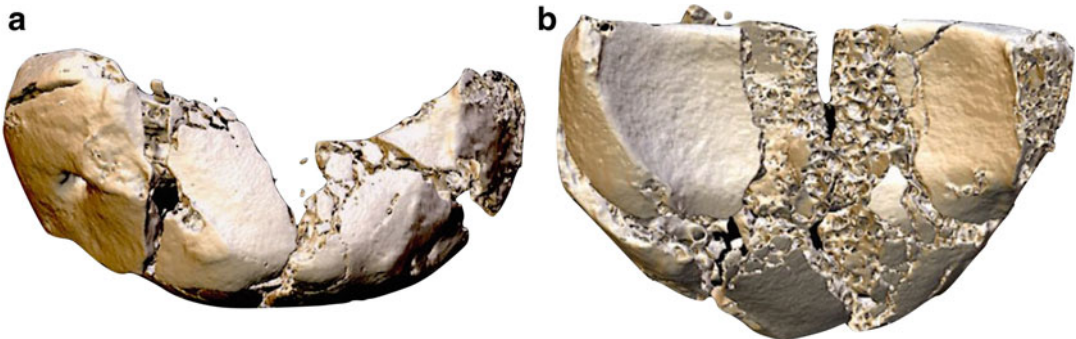


Fig. 2.7 3D micro-CT images of fractured Kienböck’s lunates in various orientations of (a) radial view, with volar and dorsal fragments, (b) distal view, with the common coronal fracture. The Kienböck’s lunate has lost the

crescent shape, and is flattened and wider. The subchondral bone plate has fragmented, producing irregular articular surfaces. Copyright Dr. Gregory Bain

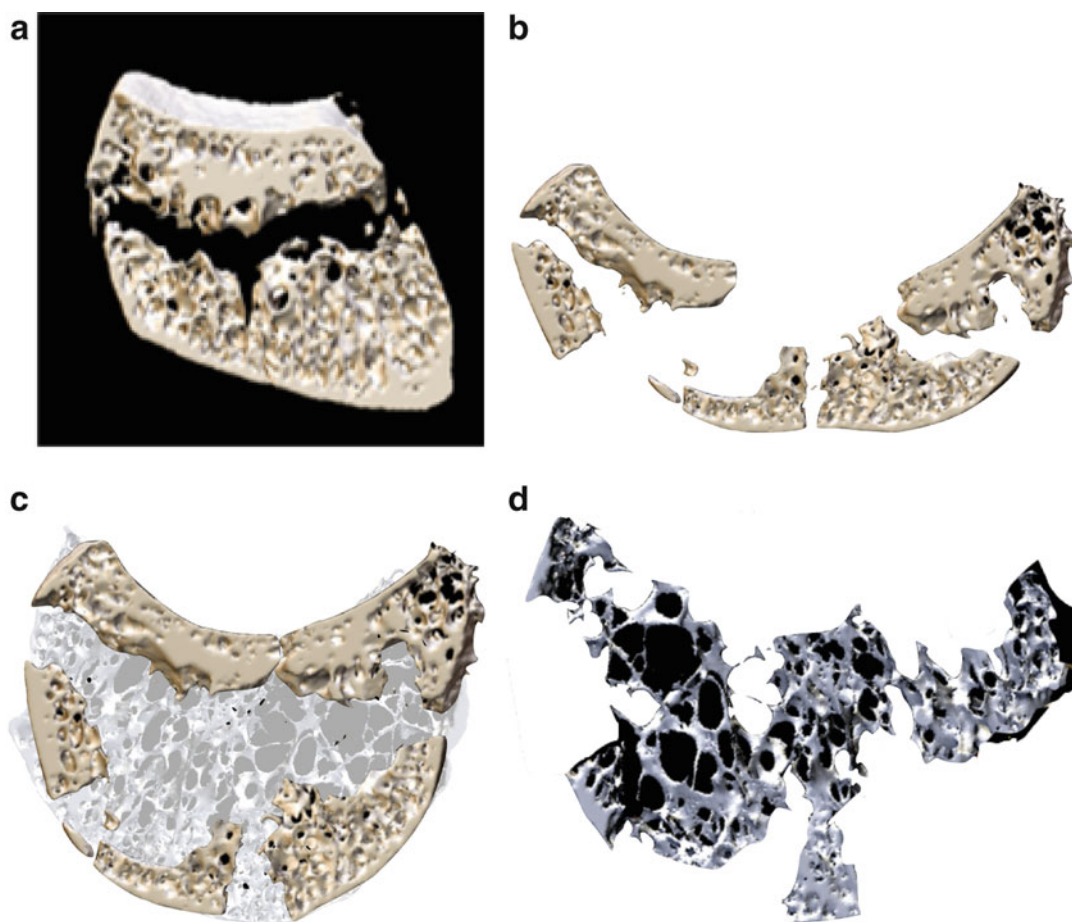


Fig. 2.8 3D micro-CT images, 1 mm thick cross sections. Kienböck's disease lunate: (a) coronal section of the lunate, consistent with a shearing fracture. (b) Sagittal section, with fragmentation of the cortical and subchondral bone plate and resorption of the spanning radial

trabeculae. (c) Reformatted sagittal section superimposed on a normal lunate. Note the multiple cortical fractures, and extensive loss of trabeculae due to fracture and resorption. (d) The proposed area of reabsorption of bone. Copyright Dr. Gregory Bain

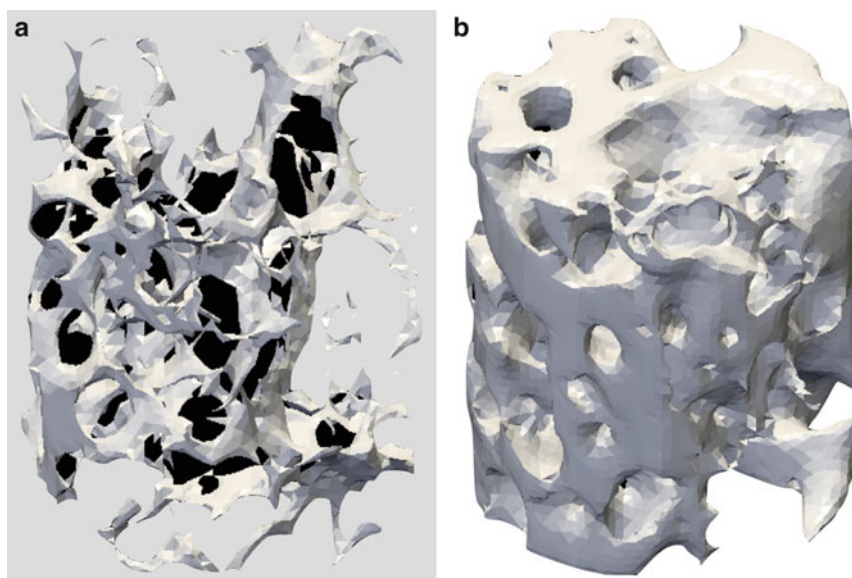


Fig. 2.9 3D morphometric analysis of the cylindrical trabecular volume of interest (3 mm diameter, 3 mm length). (a) Normal lunate and (b) Kienböck's lunate, which has

more trabeculae that are thicker. However the total bone volume of the lunate is less than the normal lunate due to bone resorption

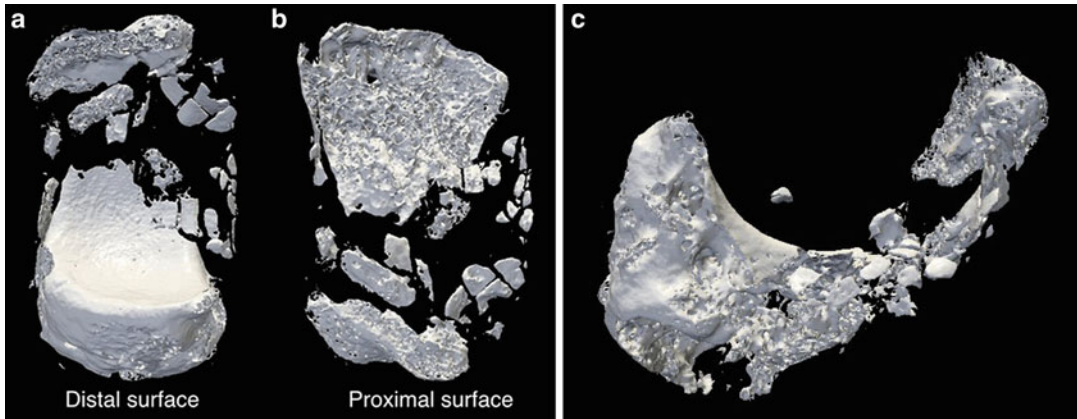
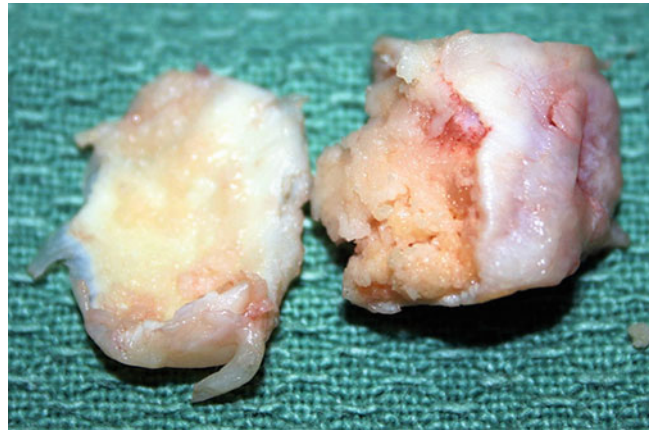


Fig. 2.10 Micro 3D CT scan images of Kienböck's lunate demonstrating extensive fragmentation and almost complete loss of the proximal subchondral bone plate, which exposes the medullary trabecular bone. This

"honeycomb" is not designed to be a load bearing surface and is therefore eroded. Distal and proximal (a, b) and lateral (c) views. Copyright Dr. Gregory Bain

Fig. 2.11 Excised Kienböck's lunate. Note the ulcerated articular surface, has lost its usual glistening surface. The subchondral bone plate has been replaced with granulation tissue. The medullary bone is fragmented, pale, and avascular. Copyright Dr. Gregory Bain



assessment of the lunate provides another insight into the morphology of the lunate (see Chap. 6 on pathology). Extensive voids can be identified, which are filled with areas of necrotic bone, scarred fibrous tissue, and cysts [16]. There are also areas of reparative tissue including granulation tissue and new bone. The new bone will respond to the forces placed upon it and take on the role of loading and supporting the capitate.

References

1. Garn SM, Rohmann CG. Variability in the order of ossification of the bony centers of the hand and wrist. *Am J Phys Anthropol.* 1960;18:219–30.
2. O'Rahilly R. Developmental deviations in the carpus and the tarsus. *Clin Orthop.* 1957;10:9–18.
3. Viegas SF, Wagner K, Patterson R, Peterson P. Medial (hamate) facet of the lunate. *J Hand Surg Am.* 1990;15(4):564–71.

4. Zapico J. Enfermedad de Kienbock. *Rev Ortop Traumatol.* 1993;37 Suppl 1:100–13.
5. Zapico J. *Malacia del semilunar.* Valladolid: Universidad de Valladolid; 1966.
6. Tatebe M, Imaeda T, Hirata H. The impact of lunate morphology on Kienbock's disease. *J Hand Surg Eur Vol.* 2015;40:534.
7. Tatebe M, Shinohara T, Okui N, Yamamoto M, Kurimoto S, Hirata H. Arthroscopic lunate morphology and wrist disorders. *Surg Radiol Anat.* 2013; 35(1):79–83.
8. Rhee PC, Moran SL, Shin AY. Effect of lunate morphology in Kienbock disease. 29th International Wrist Investigators' Workshop; 2013; Moscone West Convention Center, San Francisco, CA.
9. Owers KL, Scougall P, Dabirrahmani D, Wernecke G, Jhamb A, Walsh WR. Lunate trabecular structure: a radiographic cadaver study of risk factors for Kienbock's disease [corrected]. *J Hand Surg Eur Vol.* 2010;35(2):120–4.
10. Hülten O. Über anatomische variationen der handgelenkknochen. *Acta Radiol.* 1928;9:155–68.
11. Stahl S, Reis ND. Traumatic ulnar variance in Kienbock's disease. *J Hand Surg Am.* 1986;11(1): 95–7.
12. Gelberman RH, Bauman TD, Menon J, Akeson WH. The vascularity of the lunate bone and Kienbock's disease. *J Hand Surg Am.* 1980;5(3):272–8.
13. Chen WS, Shih CH. Ulnar variance and Kienbock's disease. An investigation in Taiwan. *Clin Orthop Relat Res.* 1990;255:124–7.
14. Tsuge S, Nakamura R. Anatomical risk factors for Kienbock's disease. *J Hand Surg Br.* 1993;18(1):70–5.
15. Low S, Bain GI, Findlay DM, Eng K, Perilli E. External and internal bone micro-architecture in normal and Kienböck's lunates: a whole-bone micro-computed tomography study. *J Orthop Res.* 2014; 32(6):826–33.
16. Bain G, Yeo CJ, Morse LP. Kienböck disease: recent advances in the basic science. Assessment and treatment. *Hand Surg.* 2015;20(3):352–65.

<http://www.springer.com/978-3-319-34224-5>

Kienböck's Disease

Advances in Diagnosis and Treatment

Lichtman, D.M.; Bain, G.I. (Eds.)

2016, XXI, 325 p. 371 illus., 159 illus. in color.,

Hardcover

ISBN: 978-3-319-34224-5